Geomechanics and Engineering, *Vol. 11*, *No. 2* (*2016*) *253-267*
DOI: http://dx.doi.org/10.12989/gae.2016.11.2.253

Study on mechanism of macro failure and micro fracture of local nearly horizontal stratum in super-large section and deep buried tunnel

Shu-cai Li [1], Jian-hua Wang [*1], Wei-zhong Chen [1,2],
Li-ping Li [1], Qian-qing Zhang [1] and Peng He [1]

[1] *Research Center of Geotechnical and Structural Engineering, Shandong University, Ji'nan 250061, Shandong, China*
[2] *State Key Laboratory of Geomechanics and Geotechnical Engineering, Institute of Rock and Soil Mechanics, Chinese Academy of Sciences, Wuhan 430071, Hubei, China*

(*Received March 12, 2015, Revised January 10, 2016, Accepted April 28, 2016*)

Abstract. The stability of surrounding rock will be poor when the tunnel is excavated through nearly horizontal stratum. In this paper, the instability mechanism of local nearly horizontal stratum in super-large section and deep buried tunnel is revealed by the analysis of the macro failure and micro fracture. A structural model is proposed to explain the mechanics of surrounding rock collapse under the action of stress redistribution and shed light on the macroscopic analytical approach of the stability of surrounding rock. Then, some highly effective formulas applied in the tunnel engineering are developed according to the theory of mixed-mode micro fracture. And well-documented field case is made to demonstrate the effectiveness and accuracy of the proposed analytical methods of mixed-mode fracture. Meanwhile, in order to make the more accurate judgment about yield failure of rock mass, a series of comprehensive failure criteria are formed. In addition, the relationship between the nonlinear failure criterion and K_{I} and K_{II} of micro fracture is established to make the surrounding rock failure criterion more comprehensive and accurate. Further, the influence of the parameters related to the tension-shear mixed-mode fracture and compression-shear mixed-mode fracture on the propagation of rock crack is analyzed. Results show that σ_3 changes linearly with the change of σ_1. And the change rate is related to β, angle between the cracks and σ_1. The proposed simple analytical approach is economical and efficient, and suitable for the analysis of local nearly horizontal stratum in super-large section and deep buried tunnel.

Keywords: instability mechanism; nearly horizontal stratum; macro failure; micro fracture; comprehensive failure criteria

1. Introduction

During the construction of tunnel, the stability of surrounding rock is affected by many factors. And the stability of surrounding rock also may be poor when the tunnel is excavated through nearly horizontal stratum. As to the analysis of stability of the local nearly horizontal stratum in super-large section and deep buried tunnel, Sun (1988) presented that the rock mass mechanics

*Corresponding author, Ph.D. Candidate, E-mail: wjh871554917@163.com

http://www.techno-press.org/?journal=gae&subpage=7 ISSN: 2005-307X (Print), 2092-6219 (Online)

medium were divided into four types such as continuous medium, crushing medium, block medium and sheet crack medium, and failure mechanism of rock mass was divided into seven kinds, i.e., tension failure, shear failure, structural element sliding along the plane of weakness, rolling failure, toppling failure, buckling failure and flexural failure. Based on the failure mode, failure criterion was also established by Sun (1988). Wang *et al*. (1984) proposed four kinds of deformation modes of surrounding rock in the soft rock tunnel, including block movement, stratum bending failure, loose failure and plastic failure.

Statistical results (Lee and Nam 2001, Zhao *et al*. 2008, Li *et al*. 2013, Yang and Qin 2014a, b, Zhang *et al*. 2014, Lin *et al*. 2015) and field investigation show that the deformation mode of rock of tunnel crossing over nearly horizontal stratum has many forms, such as flat arch, abscission layer failure, bending drum and even large area collapsed. Rock mass deformation, failure mechanism and mechanical properties are mainly controlled by rock mass structure. Local nearly horizontal strata macroscopic structure mechanics model can be established to analyze the macroscopic mechanics of surrounding rock collapse.

Due to the kinetic factor of unloading of tunnel excavation and stress redistribution, micro defects will gradually develop, causing the instability and failure of surrounding rock of tunnel. The damage types include tensile failure, tension-shear failure and compression-shear failure. Micro crack propagation of rock mass is the internal form of macro surrounding rock instability. The micro fracture mechanics is introduced to study surrounding rock stability (Tunsakul *et al*. 2013, Zhou and Qian 2013, Kazerani and Zhao 2014, Yu *et al*. 2014, 2015, Yang *et al*. 2015).

However, the previous analyses of the rock crack propagation mechanism are limited to the rock crack self propagation criterion, and there are few effective criterions on the link between micro fracture mechanism and macro failure mechanism. Therefore, there is a need to clarify the macro instability mechanism of surrounding rock, and analyze the relationship between the main parameters of crack and the surrounding rock stability based on the micro fracture mechanics criterions.

2. Macro failure of structural mechanics model

To study the stability mechanism of surrounding rock of tunnel, the local nearly horizontal strata can be simplified by the structural mechanics model. In the structural mechanics model, the vertical stress should be considered firstly. Thus, Xie (1964) proposed a formula to calculate the vertical pressure of surrounding rock, which is adopted by the Chinese Railway Tunnel Design Code (TB 10003-2005). Fig. 1(a) gives the corresponding vertical stress (σ_v)-to-buried depth(H) curve. As shown in the figure, there is a jump at the critical point of vertical stress when the buried depth changes from a state to another state.

The formula suggested by Xie (1964) should be revised, and can be rewritten as

$$\sigma_v = \begin{cases} \gamma H & (H \le B) \\ \gamma(H + K_3)(1 - K_1 H - K_2) & (B < H < B_1) \\ \gamma(B_1 + K_3)(1 - K_1 B_1 - K_2) & (H \ge B_1) \end{cases} \tag{1}$$

Where, γ is the rock density, H represents the overlying strata thickness (buried depth), B is the section width of tunnel, θ’ is the friction angle of rock mass on both sides. $K_1 = \dfrac{\tan\theta'}{B}\lambda$,

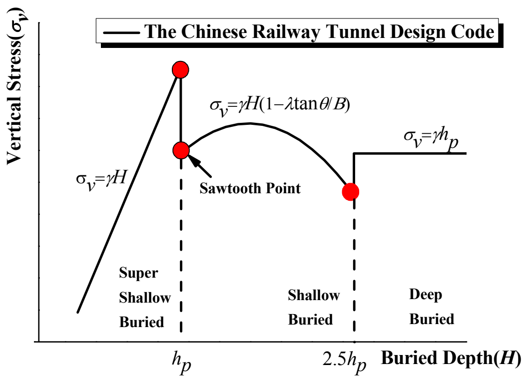

(a) The China Railway tunnel Design Code

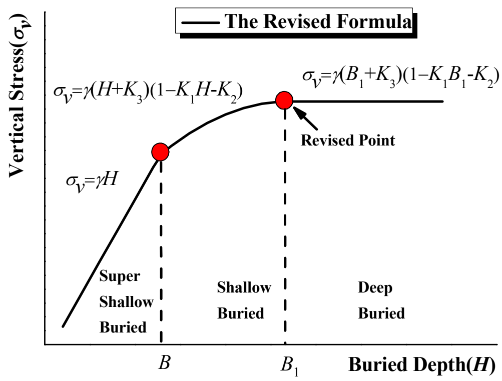

(b) The revised formula

Fig. 1 Two kinds of calculation formula of vertical stress

$K_2=\dfrac{2c}{\gamma B}$, $K_3=\dfrac{K_1B^2+K_2B}{1-K_1B-K_2}$, and $B_1=\dfrac{1-K_2-K_1K_3}{2K_1}$. Fig. 1(b) displays the revised σ_V-to-H curve.

Based on the Chinese Railway Tunnel Design Code, h_p can be expressed by

$$h_p=0.45\times 2^{s-1}\times\omega \tag{2}$$

$$\omega=1+i(B-5) \tag{3}$$

Where, h_p is the equivalent load height value, s is the grade of surrounding rock, i.e., s is taken as 3 for three grade rock, ω represents the width influence coefficient, i is the surrounding rock pressure gradient. i is adopted as 0.2 if B is less than 5m, whereas i is 0.1 when B is larger than 5 m.

To high-level analysis of the macro failure of structural mechanics model, stress distribution of the model under the action of the vertical load should be analyzed. The position of neutral axis of beam model section is related to elastic modulus and compressive modulus. Ignoring the influence of horizontal loading, σ_t and σ_c can be expressed as

$$\sigma_t=\frac{3M\left(\sqrt{E_t}+\sqrt{E_c}\right)^2}{bh^3E_c}z \tag{4}$$

$$\sigma_c=\frac{3M\left(\sqrt{E_t}+\sqrt{E_c}\right)^2}{bh^3E_t}z \tag{5}$$

Where, σ_t is the tensile stress in a certain position, σ_c represents the compressive stress, E_c is the compression modulus of rock mass, E_t is the tensile modulus, M represents the bending moment in a certain cross section, b is the average width of beam model, h is the average height of beam model, and z is the distance between a certain point and the neutral axis, and positive in the compression zone.

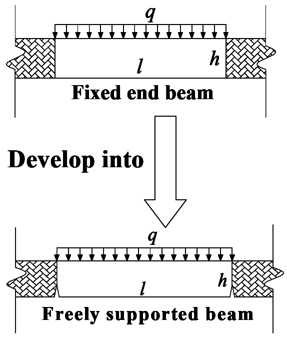

Fig. 2 Two kinds of structural mechanics model

The end of the fixed end beam model is firstly damaged when the tensile stress applied in the tensile area exceeds the tensile strength. The fixed end beam becomes supported beam model approximately. Those models are shown in Fig. 2. For a supported beam model, the center area is easy to damage. Then, the whole tension zone of single layer will damage gradually.

The plastic failure of compression zone takes place when the fixed end beam model is developed into supported beam model. The plastic failure of compression zone can be expressed as

$$f = \sqrt{J_2} - \alpha I_1 - K = 0 \tag{6}$$

Where, f is the yield function, α and K are the positive material constant, I_1 is the first stress invariable, and J_2 is the second deviatoric stress tensor invariant. If $f > 0$, the plastic damage takes place in the compression zone of structural mechanics model.

As to the plane strain problem, the τ_{xz}, α', K, I_1, and J_2 can be computed by

$$\tau_{xz} = \frac{3F_s}{2bh}\left[1 - \frac{\left(\sqrt{E_t} + \sqrt{E_c}\right)^2}{E_t h^2} z^2\right] \tag{7}$$

$$F_s = \frac{dM}{dx} \tag{8}$$

$$\alpha = \frac{\sqrt{3}\sin\varphi}{3\sqrt{3 + \sin^2\varphi}} \tag{9}$$

$$K = \frac{\sqrt{3}c\cos\varphi}{\sqrt{3 + \sin\varphi}} \tag{10}$$

$$I_1 = \sigma_x + \sigma_y + \sigma_z \tag{11}$$

$$J_2 = \frac{1}{6}\left[\left(\sigma_x - \sigma_y\right)^2 + \left(\sigma_x - \sigma_z\right)^2 + \left(\sigma_y - \sigma_z\right)^2\right] + (\tau_{xy})^2 + (\tau_{yz})^2 + (\tau_{xz})^2 \tag{12}$$

Where, F_s is the average shear force of a certain section, φ is the internal friction angle, c is the cohesion, α and K are the rock material constants related to the rock parameters of φ and c, I_1 is the first stress invariant, and J_2 is the second invariant of stress deviator tensor. τ_{xy} and τ_{yz} are adopted as 0.

3. Micro fracture of structural mechanics model

During the excavation of tunnel, the stress state of surrounding rock will convert from high dimension to low dimension and the surrounding rock stress will be redistributed. The rock mass is assumed to be as a combination of single crack unit. Actually, the analysis of the crack of surrounding rock is a three-dimensional problem. However, due to the complexity of the analysis of 3-D crack, the analysis on the two-dimensional crack is considered in the present paper.

The type of crack tip propagation is mostly mixed-mode propagation because of the complexity of stress distribution surrounding rock. In general, the mixed-mode propagation includes compression-shear mixed-mode propagation and tension-shear mixed-mode propagation. In the paper, the mechanism of micro tension-shear mixed-mode fracture and compression-shear mixed-mode fracture under the secondary state of stress is analyzed.

3.1 Tension-shear mixed-mode fracture

In the cracked rock mass model, closed crack is under the control of the major principal stresses σ_1 and the minor principal stresses σ_3. The angle between the cracks and the major principal stress σ_1 is defined as β, The closed cracks length are $2a$. The cracked rock mass model is shown in Fig. 3. The τ and σ_n can be expressed as

$$\tau = -\frac{\sigma_1 - \sigma_3}{2}\sin 2\beta \tag{13}$$

$$\sigma_n = -\left(\frac{\sigma_1 + \sigma_3}{2} - \frac{\sigma_1 - \sigma_3}{2}\right)\cos 2\beta \tag{14}$$

Where, σ_n is the normal stress of crack surface, and τ is the shear stress of crack surface.

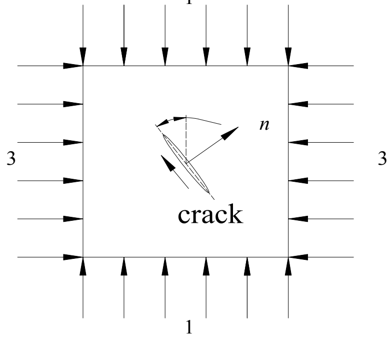

Fig. 3 Cracked rock mass model

$$\begin{matrix}\sigma_1 \\ \sigma_3\end{matrix} = \frac{\sigma_x + \sigma_z}{2} \pm \sqrt{(\frac{\sigma_x - \sigma_z}{2})^2 + \tau_{xz}{}^2} \tag{15}$$

The directions which are parallel and perpendicular to the horizontal axis of tunnel are defined as *X*-axis and *Y*-axis, respectively. Then, *Z*-axis is the direction which is perpendicular to the plane formed by *X*-axis and *Y*-axis.

For mixed-mode fracture criterion, there are maximum circumferential stress criterion, strain energy density factor theory and energy release rate theory. The calculation of these criterions is generally tedious, which is unsuitable for engineering application. The simple propagation criterion can be expressed by the following form

$$K_{\mathrm{I}} + K_{\mathrm{II}} = K_{\mathrm{IC}} \tag{16}$$

Where, K_{IC} is the toughness of mode I fracture. K_{I} and K_{II} are the crack tip stress intensity factors for type I and type II fracture, respectively. K_{I} and K_{II} can be expressed as

$$K_{\mathrm{I}} = \sigma_n \sqrt{\pi a} \tag{17}$$

$$K_{\mathrm{II}} = \tau \sqrt{\pi a} \tag{18}$$

For the fracture mechanics, tensile stress is positive and compressive stress is negative. For the rock mechanics, compressive stress is positive and tensile stress is negative.

According to Eqs. (13), (14) and (16), the tension-shear mixed-mode fracture can be demonstrated as

$$\left(\frac{\sigma_1 + \sigma_3}{2} - \frac{\sigma_1 - \sigma_3}{2}\cos 2\beta\right) + \left|\frac{\sigma_1 - \sigma_3}{2}\sin 2\beta\right| + \frac{K_{\mathrm{IC}}}{\sqrt{\pi a}} = 0 \tag{19}$$

3.2 Compression-shear mixed-mode fracture

When the normal stress of a crack surface is compressive stress, this crack propagation problem belongs to compression-shear mixed-mode propagation in fracture mechanics. The original opened crack surface will gradually close with the compression stress. The closed crack is uniform contact and transfer of normal stress and shear stress. The shear role effective shear stress in the crack face results the compression-shear failure of surrounding rock. The value of effective shear stress is nominal shear stress applied in the crack surface minus the friction resistance. Friction resistance of crack surface can be derived from the Mohr-Coulomb criterion.

$$\tau_f = c + \sigma_n \tan\varphi \tag{20}$$

$$\tau' = |\tau| - \tau_f \tag{21}$$

Where, τ' is the effective shear stress, $|\tau|$ is the absolute value of nominal shear stress, τ_f is the friction resistance.

Based on the compression-shear fracture criterion derived from regression analysis of test, a criterion is proposed to simulate the compression-shear properties of rocks, which can be expressed as

$$\lambda' K_{\mathrm{I}} + |K_{\mathrm{II}}| = K_{\mathrm{IIC}} \tag{22}$$

Where, λ' is the compression-shear parameter which is related to the compression-shear properties of rock. λ' is generally determined by experiment. K_{IIC} is mode II fracture toughness under compression-shear condition.

According to Eqs. (13), (14) and (22), the compression-shear mixed-mode fracture can be demonstrated as

$$-(\lambda' - \tan\varphi)\left(\frac{\sigma_1 + \sigma_3}{2} - \frac{\sigma_1 - \sigma_3}{2}\cos 2\beta\right) + \left|\frac{\sigma_1 - \sigma_3}{2}\sin 2\beta\right| = c + \frac{K_{\mathrm{IIC}}}{\sqrt{\pi a}} \tag{23}$$

4. Comprehensive failure criteria

It is considered that mixed-mode propagation leads to local nearly horizontal strata instability with the instability analysis of structure mechanics model. Therefore, the cracks propagation process is essentially the process of rock failure. There is a certain correlation between the micro fracture and the macro-failure. The relationship between the micro fracture and the macro failure should be established to reflect the instability of rock failure according to the microscopic crack propagation mechanism.

Based on the nonlinear Mohr-Coulomb criterion and Druker-Prager failure criterion, the relationship between macroscopic tension-shear failure and compression-shear failure and K_{I} and K_{II} of micro fracture is analyzed. Then, comprehensive failure criterion of tension-shear failure and compression-shear failure is established.

4.1 Crack-tip stress field

For mixed mode I-II crack model shown in Fig. 4, the stress field near the crack tip is superimposed by type I fracture and type II fracture, which can be demonstrated as

$$\sigma_r = \frac{1}{2\sqrt{2\pi r}}\left[K_{\mathrm{I}}\,(3-\cos\theta)\cos\frac{\theta}{2} + K_{\mathrm{II}}\,(3\cos\theta - 1)\sin\frac{\theta}{2}\right] \tag{24}$$

$$\sigma_\theta = \frac{1}{2\sqrt{2\pi r}}\cos\frac{\theta}{2}\left[K_{\mathrm{I}}\,(1+\cos\theta) - 3K_{\mathrm{II}}\,\sin\theta\right] \tag{25}$$

$$\tau_{r\theta} = \frac{1}{2\sqrt{2\pi r}}\cos\frac{\theta}{2}\left[K_{\mathrm{I}}\,\sin\theta + K_{\mathrm{II}}\,(3\cos\theta - 1)\right] \tag{26}$$

Where, θ is the angle between a certain point of crack and the polar axis, and r is the distance between the certain point of crack and the polar axis.

The transformation relationship between the rectangular coordinate system and the polar coordinates system can be demonstrated as

$$\sigma_r = \frac{\sigma_x + \sigma_z}{2} + \frac{\sigma_x - \sigma_z}{2}\cos 2\theta + \tau_{xz}\sin 2\theta \tag{27}$$

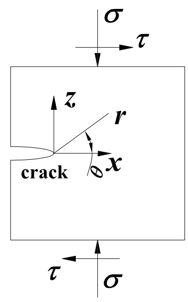

Fig. 4 Crack-tip stress field

$$\sigma_\theta = \frac{\sigma_x + \sigma_z}{2} - \frac{\sigma_x - \sigma_z}{2}\cos 2\theta - \tau_{xz}\sin 2\theta \tag{28}$$

$$\tau_{r\theta} = \tau_{xz}\cos 2\theta - \frac{\sigma_x - \sigma_z}{2}\sin 2\theta \tag{29}$$

Then, the crack-tip stress in the rectangular coordinate system can be rewritten as

$$\sigma_x = \frac{K_{\mathrm{I}}}{\sqrt{2\pi r}}\cos\frac{\theta}{2}\left(1 - \sin\frac{\theta}{2}\sin\frac{3\theta}{2}\right) - \frac{K_{\mathrm{II}}}{\sqrt{2\pi r}}\sin\frac{\theta}{2}\left(2 + \cos\frac{\theta}{2}\cos\frac{3\theta}{2}\right) \tag{30}$$

$$\sigma_z = \frac{K_{\mathrm{I}}}{\sqrt{2\pi r}}\cos\frac{\theta}{2}\left(1 + \sin\frac{\theta}{2}\sin\frac{3\theta}{2}\right) + \frac{K_{\mathrm{II}}}{\sqrt{2\pi r}}\sin\frac{\theta}{2}\cos\frac{\theta}{2}\cos\frac{3\theta}{2} \tag{31}$$

$$\tau_{xz} = \frac{K_{\mathrm{I}}}{\sqrt{2\pi r}}\sin\frac{\theta}{2}\cos\frac{\theta}{2}\cos\frac{3\theta}{2} + \frac{K_{\mathrm{II}}}{\sqrt{2\pi r}}\cos\frac{\theta}{2}\left(1 - \sin\frac{\theta}{2}\sin\frac{3\theta}{2}\right) \tag{32}$$

According to the Druker-Prager failure criteria, the relationship among K_{I}, K_{II} and I_1, J_2 have been established by Zhou *et al*. (2007), which can be described as

$$I_1 = \frac{2\left(K_{\mathrm{I}}\cos\frac{\theta}{2} - K_{\mathrm{II}}\sin\frac{\theta}{2}\right)}{\sqrt{2\pi r}} \tag{33}$$

$$\begin{aligned} J_2 = &\frac{7K_{\mathrm{I}}^2 + 19K_{\mathrm{II}}^2 + 4(K_{\mathrm{I}}^2 - K_{\mathrm{II}}^2)\cos\theta - 8K_{\mathrm{I}}K_{\mathrm{II}}\sin\theta}{48\pi r} \\ &+ \frac{12K_{\mathrm{I}}K_{\mathrm{II}}\sin 2\theta - 3(K_{\mathrm{I}}^2 - 3K_{\mathrm{II}}^2)\cos 2\theta}{48\pi r} \end{aligned} \tag{34}$$

$$f_1(K_{\mathrm{I}}, K_{\mathrm{II}}, \theta) = K_{\mathrm{I}}\cos 2\theta - K_{\mathrm{II}}\sin\frac{\theta}{2} \tag{35}$$

$$f_2(K_{\mathrm{I}},K_{\mathrm{II}},\quad \theta)=7K_{\mathrm{I}}^{2}+19K_{\mathrm{II}}^{2}+4(K_{\mathrm{I}}^{2}-K_{\mathrm{II}}^{2})\cos\theta \\ +12K_{\mathrm{I}}K_{\mathrm{II}}\sin 2\theta-3(K_{\mathrm{I}}^{2}-3K_{\mathrm{II}}^{2})\cos 2\theta-8K_{\mathrm{I}}K_{\mathrm{II}}\sin\theta \tag{36}$$

4.2 Nonlinear comprehensive failure criterion

The Mohr-Coulomb criterion and the Druker-Prager criterion are commonly used to analyze the plastic failure of surrounding rock in the buried tunnel. The Mohr envelop in the two criterions are generally be fitted by a straight line, which leads to the two criterions being suitable for the compression-shear failure condition. And the two criterions have a poor applicability in tension-shear failure condition. However, the nonlinear models show a better applicability for all the two failure conditions. And the nonlinear model can be described by the parabolic yield criterion (Baker 2004, Li *et al*. 2005, Das and Basudhar 2009, Youn and Tonon 2010, Nazife and David 2012).

According to principle of the nonlinear model, the Mohr-Coulomb yield criterion can be re-described as a two-parameter parabolic yield criterion, which can be expressed as

$$f=a\tau^2+\sigma-b \tag{37}$$

The values of the parameters of a, b, and m can be computed as

$$\begin{cases} a=\dfrac{\left(1+\sqrt{m+1}\right)^2}{mR_c} \\ b=R_t \\ m=\dfrac{R_c}{R_t} \end{cases} \tag{38}$$

Where, R_c is the uniaxial compressive strength, and R_t is the uniaxial tensile strength.

For the principal stress, two parameter parabolic yield criterion can be solved by using the following constraint.

$$\begin{cases} \dfrac{a(\sigma_1-\sigma_3)}{4}=\dfrac{(\sigma_1+\sigma_3)}{2}+R_t-\dfrac{1}{4a}\left(\sigma_1>-R_t+\dfrac{1}{a}\right) \\ \sigma_3=-R_t\left(\sigma_1\le -R_t+\dfrac{1}{a}\right) \end{cases} \tag{39}$$

$$\begin{bmatrix}\sigma_1\\ \sigma_2\\ \sigma_3\end{bmatrix}=\frac{2}{\sqrt{3}}\sqrt{J_2}\begin{bmatrix}\sin(\theta_\sigma+\frac{2}{3}\pi)\\ \sin(\theta_\sigma)\\ \sin(\theta_\sigma-\frac{2}{3}\pi)\end{bmatrix}+\begin{bmatrix}\sigma_m\\ \sigma_m\\ \sigma_m\end{bmatrix} \tag{40}$$

$$\sigma_m=\frac{I_1}{3} \tag{41}$$

Where, σ_m is hydrostatic stress tensor.

For the stress invariant, two parameter parabolic yield criterion can be solved by using the following constraint.

$$\begin{cases} f = a\cos^2\theta_\sigma J_2 + \dfrac{\sqrt{J_2}}{\sqrt{3}}\sin\theta_\sigma - \dfrac{2}{3}I_1 - R_t + \dfrac{1}{4a} = 0\left(\sigma_1 > -R_t + \dfrac{1}{a}\right) \\ f = \dfrac{2}{\sqrt{3}}\sqrt{J_2}\sin\left(\theta_\sigma - \dfrac{2\pi}{3}\right) + \dfrac{I_1}{3} + R_t = 0\left(\sigma_1 \le -R_t + \dfrac{1}{a}\right) \end{cases} \tag{42}$$

Where, θ_σ is the Lode angles. Lode angles can be approximately assumed to be a constant value in practice.

Substituting Eq. (35) and (36) into Eq. (42), the value of f can be calculated by

$$\begin{cases} f = \dfrac{a\cos^2\theta_\sigma f_2(K_\mathrm{I},K_\mathrm{II},\theta)}{48\pi r} + \dfrac{\sqrt{f_2(K_\mathrm{I},K_\mathrm{II},\theta)}}{12\sqrt{\pi r}}\sin\theta_\sigma - \dfrac{4f_1(K_\mathrm{I},K_\mathrm{II},\theta)}{3\sqrt{2\pi r}} - R_t + \dfrac{1}{4a} = 0\left(\sigma_1 > -R_t + \dfrac{1}{a}\right) \\ f = \dfrac{\sqrt{f_2(K_\mathrm{I},K_\mathrm{II},\theta)}}{6\sqrt{\pi r}}\sin\left(\theta_\sigma - \dfrac{2\pi}{3}\right) + \dfrac{2f_1(K_\mathrm{I},K_\mathrm{II},\theta)}{3\sqrt{2\pi r}} + R_t = 0\left(\sigma_1 \le -R_t + \dfrac{1}{a}\right) \end{cases} \tag{43}$$

Based on the suggestion of Li and Yin (2010), comprehensive failure criteria of the Druker-Prager criteria can also be re-expressed as

$$f = (J_2 + a'^2k^2)^{\frac{1}{2}} + \alpha I_1 - k = 0 \tag{44}$$

Where, $a' = 1 - \dfrac{\alpha\sigma_t}{k}$, whose value is in the range 0 to 1.

Substituting Eqs. (35) and (36) into Eq. (44), it can be concluded that

$$8\sqrt{3}\alpha f_1(K_\mathrm{I},K_\mathrm{II},\theta) + \sqrt{2f_2(K_\mathrm{I},K_\mathrm{II},\theta) + 96\pi r a'^2k^2} - 4\sqrt{6\pi r}k = 0 \tag{45}$$

In the comprehensive failure criterion, the damage of structural mechanics model is connected with K_I, K_II and the initial crack angle (θ). By the established comprehensive failure criterions, the effectiveness and accuracy of the proposed analytical Eqs. (19) and (23) have been verified. In practical engineering, the nonlinear comprehensive failure criterions (43) and (45) are used to judge whether damage occurs firstly, and then the Eqs. (19) and (23) are used to judge what kind of damage. The limitations of the comprehensive failure criterion need to be further studied in view of the practical engineering.

5. Engineering application

5.1 Project background

Chengdu-Lanzhou Railway in China is selected to check the reliability of the present paper. The NATM is required to apply in this tunnel. Auxiliary advance support measures are used such as advance grouting pipe, anchor bolt and advanced pipe shed principle. Composite lining measure is used in this tunnel which includes steel arch support, steel mesh reinforcement, bolt, and wet spraying concrete. According to the design requirements, shotcrete thickness is 27 cm. Benching tunneling construction method is adopted. During the slag process of D2K0+160~152, local nearly horizontal stratum near the vault is exposed for about one day, which leads to the collapse. According to the design and literature, φ is about 15°, α is 0.6 m and C is 80 kPa. The local nearly horizontal stratum and collapse site are shown in Fig. 5 and Fig. 6.

The vertical stress of nearly horizontal stratum can be determined based on Eq. (1). Then, according to Eqs. (4) and (5) and the engineering design information, the σ_1 and σ_3 can be calculated easily. And the σ_n and τ can also be calculated based on the Eqs. (13) and (14). For a rock unity near the tunnel vault with β being 60°, σ_1 is 1.4 MPa, σ_3 is 0.1 MPa, σ_n is 1.1 MPa and τ is 0.56 MPa in the compression-shear zone. σ_1 is 0.1 MPa, σ_3 is -1.1 MPa, σ_n is -0.2 MPa and τ is 0.52 MPa in the tension-shear zone .

According to Eqs. (17) and (18), K_{I} is 1.5 MPa·m$^{1/2}$ and K_{II} is about 0.77 MPa·m$^{1/2}$ in the compression-shear zone and K_{I} is -0.27 MPa·m$^{1/}$ and K_{II} is about 0.71 MPa·m$^{1/2}$ in the tension-shear zone. Then, by the analysis of failure criterions shown in Eqs. (43) and (45), it can be concluded that rock mass unit is destroyed. Combined with engineering experience and design information, K_{IC} is 0.46 MPa·m$^{3/2}$ and K_{IIC} is about 0.368 MPa·m$^{1/2}$, the tension-shear failure and compression-shear failure can be judged by Eqs. (19) and (23), respectively.

From the above calculated process, it can be concluded that the process is very complex. The relationship among σ_1, σ_3 and β will be discussed to in the next section to support a simple method to judge the occurrence of instability.

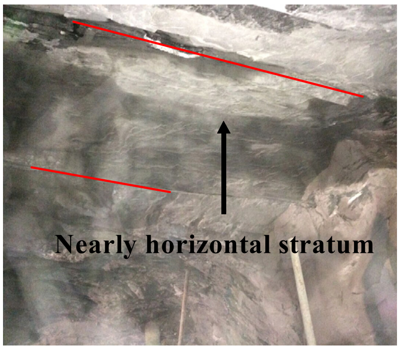

Fig. 5 Local nearly horizontal stratum near tunnel vault

Fig. 6 Collapsing of tunnel

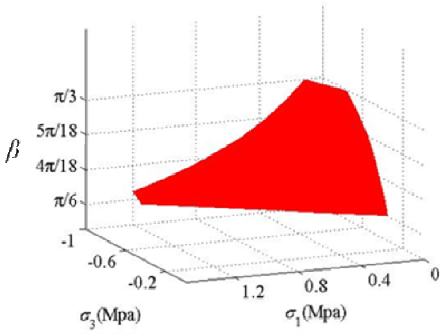

Fig. 7 3-D σ_1-σ_3-β diagram of tension-shear mixed-mode fracture

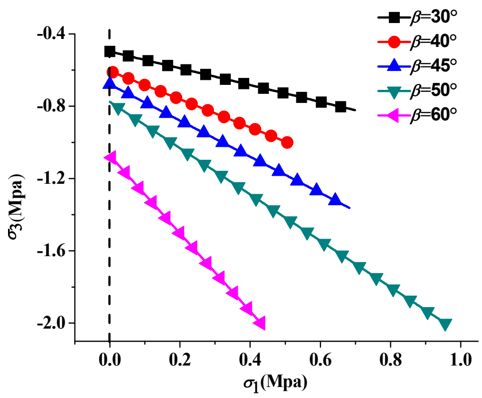

Fig. 8 σ_1-σ_3 curves of tension-shear mixed-mode fracture

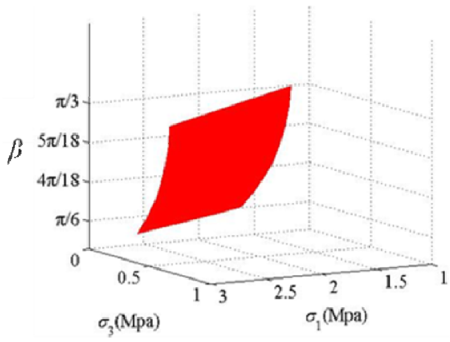

Fig. 9 3-D σ_1-σ_3-β diagram of compression-shear mixed-mode fracture

5.2 Parameters analysis

When the rock cracks are under the tension-shear condition, the relationships σ_1, σ_3 and β are shown in Figs. 7 and 8. It can be seen from Fig. 8, the value of σ_3 decreases linearly with the increase of σ_1. And the decrease rate of σ_3 is proportion to β.

When the rock cracks are under the compression-shear condition, the relationships σ_1, σ_3 and β are shown in Figs. 9 and 10 (Partial data for σ_3 is tensile stress are not shown in Fig. 10). It can

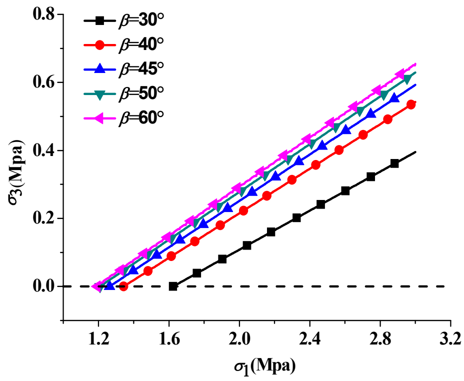

Fig. 10 σ_1-σ_3 curves of compression-shear mixed-mode fracture

be seen from Fig. 10, the value of σ_3 increases linearly with the increase of σ_1. And the increase rate of σ_3 is proportion to β.

From Figs. 8 and 10, it can be also seen that the change relationship among $\sigma_{1,}$ σ_3 and β can be used to judge the tension-shear failure or the compression-shear failure directly.

6. Conclusions

In this paper, the instability mechanism of local nearly horizontal stratum in super-large section and deep buried tunnel is systematically studied from two aspects of macro failure and micro fracture. The study improves understanding of the mechanics of surrounding rock collapse under the action of stress redistribution and sheds light on the macroscopic analytical approach of the stability of surrounding rock using the proposed structural model. Furthermore, some highly effective formulas applied in the tunnel engineering are developed using the theory of mixed-mode micro fracture. And well-documented field case is made to demonstrate the effectiveness and accuracy of the proposed analytical methods of mixed-mode fracture. Meanwhile, in order to make the more accurate judgment about yield failure of rock mass, a series of comprehensive failure criteria are formed. The relationship between the nonlinear failure criterion and K_{I} and K_{II} of micro fracture is established. That makes the surrounding rock failure criterion more comprehensive and accurate.

Further study is conducted to analyze the influence of the parameters related to the tension-shear mixed-mode fracture and compression-shear mixed-mode fracture on the propagation of rock crack. The σ_3 changes linearly with the increase of σ_1. And the change rate of the σ_3 is related to β, angle between the cracks and σ_1. According to the relationship among σ_1, σ_3 and β in this stage, the kind of the failure can be judged easily.

The proposed simple analytical approach is economical and efficient, and suitable for the analysis of local nearly horizontal stratum in super-large section and deep buried tunnel.

Acknowledgments

This work was supported by the National Program on Key Basic Research Project of China (973 Program) (No. 2013CB036000), Nation Natural Science Foundation of China (General Program)

(No. 51479106), the Natural Science Foundation of Shandong Province of China (NO. 2014ZRE27303). The authors would like to express appreciation to the reviewers for their valuable comments and suggestions that helped to improve the quality of the paper.

References

Baker, R. (2004), "Nonlinear Mohr envelopes based on triaxial data", *J. Geotech. Geoenviron. Eng.*, **130**(5), 498-506.

Das, S.K. and Basudhar, P.K. (2009), "Comparison of intact rock failure criteria using various statistical methods", *Acta Geotech.*, **4**(3), 223-231.

Kazerani, T. and Zhao, J. (2014), "A microstructure-based model to characterize micromechanical parameters controlling compressive and tensile failure in crystallized rock", *Rock Mech. Rock Eng.*, **47**(2), 435-452.

Lee, I.M. and Nam, S.W. (2001), "The study of seepage forces acting on the tunnel lining and tunnel face in shallow tunnels", *Tunn. Undergr. Space Technol.*, **16**(1), 31-40.

Li, P.E. and Yin, Y.Q., (2010), "Modification of Drucker-Parger criterion in tensile shear region", *Chinese J. Rock Mech. Eng.*, **29**(supp1), 3029-3033.

Li, C.G., Zheng, H., Ge, X.R. and Wang, S.L. (2005), "Research on two-parameter parameter parabolic mohr strength criterion and its damage regularity", *Chinese J. Rock Mech. Eng.*, **24**(24), 4428-4433.

Li, S.C., Hu, C. and Li, L.P. (2013), "Bidirectional construction process mechanics for tunnels in dipping layered formation", *Tunn. Undergr. Space Technol.*, **36**, 57-65.

Lin, P., Liu, H.Y. and Zhou, W.Y. (2015), "Experimental study on failure behaviour of deep tunnels under high in-situ stresses", *Tunn. Undergr. Space Technol.*, **46**, 28-45.

Nazife, E. and David, J.W. (2012), "Experimental, numerical and analytical studies on tensile strength of rocks", *Int. J. Rock Mech. Mining Sci.*, **48**(1), 21-30.

Sun, G.Z. (1988), *Rock Mass Structure Mechanics*, Science Press, Beijing, China.

The Professional Standards Compilation Group of People's Republic of China (2005), TB 10003—2005, Code for design on tunnel of railway, Beijing, China.

Tunsakul, J., Jongpradist, P., Kongkitkul, W., Wonglert, A. and Youwai, S. (2013), "Investigation of failure behavior of continuous rock mass around cavern under high internal pressure", *Tunn. Undergr. Space Technol.*, **34**, 110-123.

Wang, S.J., Yang, Z.F. and Liu, Z.H. (1984), *Underground Engineering Rock Mass Stability Analysis*, Science Press, Beijing, China.

Xie, J.X. (1964), "Earth pressure on shallow burial tunnel", *China Civil Eng. J.*, **10**(6), 58-70.

Yang, X.L. and Qin, C.B. (2014a), "Limit analysis of rectangular cavity subjected to seepage forces based on Hoek-Brown failure criterion" *Geomech. Eng.*, **6**(5), 503-515.

Yang, X.L. and Qin, C.B. (2014b), "Upper bound limit analysis of roof collapse in shallow tunnels with arbitrary cross sections under condition of seepage force", *J. Cent. South. Univ.*, **21**(11), 4338-4343.

Yang, J.P., Chen, W.Z. and Yang, D.S. (2015), "Numerical determination of strength and deformability of fractured rock mass by FEM modeling", *Comput. Geotech.*, **64**, 20-31.

Youn, H. and Tonon, F. (2010), "Multi-stage triaxial test on brittle rock", *Int. J. Rock Mech. Mining Sci.*, **47**(4), 678-684.

Yu, Q.L., Zhu, W.C. and Tang, C.A. (2014), "Impact of rock microstructures on failure processes-Numerical study based on DIP technique", *Geomech. Eng., Int. J.*, **7**(4), 375-401.

Yu, S., Zhu, W.S., Yang, W.M., Zhang, D.F. and Ma, Q.S. (2015), "Rock bridge fracture model and stability analysis of surrounding rock in underground cavern group", *Struct. Eng. Mech., Int. J.*, **53**(3), 481-495.

Zhao, Y.L., Cao, P., Wen, Y.D., Yang, H. and Li, J.T. (2008), "Damage fracture failure mechanism of compressive-shear rock cracks under seepage pressure", *J. Cent. South. Univ.*, **39**(4), 838-844.

Zhang, C.P., Han, K.H. and Fang, Q. (2014), "Functional catastrophe analysis of collapse mechanisms for deep tunnels based on the Hoek-Brown failure criterion", *J. Zhejiang Univ-Sc. A*, **15**(9), 723-731.

Zhou, X. and Qian, Q. (2013), "Zonal disintegration mechanism of the microcrack-weakened surrounding rock mass in deep circular tunnels", *J. Min. Sci.*, **49**(2), 210-219.
Zhou, J.W., Xu, W.Y. and Shi, C. (2007), "Investigation on compression-shear fracture criterion of rock based on rock based on failure criteria", *Chinese J. Rock Mech. Eng.*, **26**(6), 1194-1200.

CC